A STUDY OF FINITE DIFFERENCE METHODS AS APPLIED TO NONLINEAR HYPERSONIC VISCOUS BOUNDARY LAYER EQUATIONS

by: A. L. Chang and H. K. Cheng

Contract No. Nonr 2653(00)
Report No. AF-1285-A-9
March 1963

CORNELL AERONAUTICAL LABORATORY, INC.
OF CORNELL UNIVERSITY, BUFFALO 21, N. Y.

CORNELL AERONAUTICAL LABORATORY, INC.
BUFFALO 21, NEW YORK

CAL REPORT NO. AF-1285-A-9

A STUDY OF FINITE-DIFFERENCE METHODS AS APPLIED TO HYPERSONIC VISCOUS SHOCK-LAYER EQUATIONS

MARCH 1963

AUTHORS: Angela L. Chang
A. L. Chang

H. K. Cheng
H. K. Cheng

APPROVED BY:
A. Hertzberg, Head
Aerodynamics Research Dept.

FOREWORD

The study herein reported is part of the program of research on Viscous Flow sponsored by the U.S. Navy through the Office of Naval Research under Contract Nonr 2653(00). The analytic series solution used in the analyses was obtained from an earlier related study sponsored by the U. S. Air Force through the Office of Scientific Research under Contract AF 49(638)-952. The authors would like to take this opportunity to thank Mr. Harvey Selib of the Systems Research Department of Cornell Aeronautical Laboratory for his assistance in programming the numerical computations as well as many helpful suggestions.

TABLE OF CONTENTS

LIST OF ILLUSTRATIONS

LIST OF SYMBOLS

C	constant in the linear viscosity and temperature relation $\frac{\mu}{\mu_\infty} = C\frac{T}{T_\infty}$
c_F	$\equiv \mu \frac{\partial u}{\partial y} \Big/ \frac{1}{2}\rho_\infty U_\infty^2$, coefficient of skin friction
c_H	$\equiv K\frac{\partial T}{\partial y} \Big/ \rho_\infty U_\infty (H_\infty - H_w)$, coefficient of heat transfer
H	specific total enthalpy
m, n	$\equiv \frac{\bar{x}}{\Delta\bar{x}}$, $\frac{\bar{\psi}}{\Delta\bar{\psi}}$, coordinates of the grid points
Re_x	$\equiv \rho_\infty U_\infty x / \mu_0$, a Reynolds number
T_*	reference temperature used in the determination of $C = \frac{\mu_*}{\mu_\infty}\frac{T_\infty}{T_*}$ See Eq. (31)
U_∞	free-stream velocity
u	the velocity component along x-direction
$\bar{u}$	$\equiv \frac{u}{U_\infty \cos\beta}$, a non-dimensionalized velocity component
W	$\equiv \frac{\bar{u}^2}{2} = \frac{1}{2}\left(\frac{u}{U_\infty \cos\beta}\right)^2$
x, y	distances along and normal to the surface, respectively
$\bar{x}$	$\equiv \frac{\rho_\infty x}{\mu_\infty U_\infty C \cos\beta} = \varepsilon Re_b \sec\beta \left(\frac{\mu_0}{\mu_*}\frac{T_*}{T_0}\right)$
z	distance of the body surface from the axis of symmetry
β	the shock angle
ε	$= \frac{\gamma - 1}{2\gamma}$
γ	specific-heat ratio
η	the similarity variable defined in Eq. (30)
μ	viscosity

ρ_∞	free-stream density
ψ	stream function
$\bar{\psi}$	$\equiv \psi / \rho_\infty U_\infty \bar{z} (r \bar{z})^\nu$
ν	a parameter which is zero for a wedge and unity for a cone

Subscripts

$0, w, \infty, *$	pertaining to the stagnation, surface, free-stream, and reference conditions
m, η	pertaining to the conditions at the grid points

ABSTRACT

The problem of numerical integration of the parabolic differential equations of viscous shock-layer theory are studied. Three methods are considered: the standard explicit and implicit schemes, as well as the explicit scheme of DuFort and Frankel. The relative merit and efficiency of these methods are discussed in terms of numerical solutions carried out for the shock layer on a cone.

Because of the singularity in the governing equation, the mesh size associated with the difference approximation must be progressively refined as the leading-edge is approached. This, in practice, places a severe handicap on all difference methods, particularly the explicit scheme which is already restricted by the requirement of stability. The examples worked out here for flows over cones confirm that the implicit and DuFort-Frankel explicit schemes, which are not subject to the stability requirement, are more effective. Although the difference between the two latter schemes is not large in this example, the discussion reveals that the implicit scheme, which is subject to neither the stability nor the convergence requirement, is much more efficient and accurate in problems involving non-vanishing pressure gradients.

I. INTRODUCTION

There are many methods for obtaining numerical solutions to nonlinear partial differential equations of hyperbolic or parabolic type. The following study concerns the application of numerical methods to the study of the low-density hypersonic flow based on the mathematical formulation of Ref. 1, in which the system of governing equations is reduced to one of the parabolic type, similar to those of the boundary-layer theory.

In preparation for a more general attack, the present investigation is made with the objective of examining the applicability of certain finite-difference techniques to the hypersonic shock-layer theory. For this purpose, analyses and discussions will be made only for the simplest example, that of hypersonic flow over a cone at low Reynolds number. In this case, under the assumption of a unit Prandtl number, the governing equations are reducible to a single parabolic equation, but the solution is no longer self-similar as in the boundary-layer theory because of the modified outer boundary condition. Near the cone apex, an analytic development in ascending powers of the distance from the apex is valid; while far downstream, an asymptotic, self-similar solution corresponding to the classical boundary-layer theory exists. The finite-difference methods provide a valid transition between the two solutions. The agreement with these two solutions at small and large distances provides a check of the accuracy of the finite-difference methods.

In the method of finite differences, the derivatives are replaced by the quotients of the differences, and the partial differential equations are satisfied approximately at a finite number of grid or lattice points. For an initial-value problem pertaining to the parabolic and hyperbolic equations, solution by

forward integration is possible, and the solution to the difference equation can be determined in terms of previously obtained values at certain preceding stations or grid line. By employing sufficiently small spacing between grid points, and with the aid of a high-speed digital computer, one may obtain a numerical solution with high accuracy.

The manner in which the difference quotients are formed and the equations approximated gives rise to a variety of difference methods.[2, 3] The simplest and most commonly known of these is the standard explicit scheme by which each unknown quantity is determined explicitly in terms of values obtained previously at a preceding station.[2, 3] This method is, however, restricted by the stability requirements. Another scheme introduced by DuFort and Frankel[2, 3, 4] is also explicit, in that each unknown value of the solution is determined explicitly with the known values at two preceding stations in a specific manner. Although this method is generally stable, the question of convergence may become a critical problem. In an implicit scheme,[2, 3] each unknown value of the solution is not determined explicitly in terms of the known quantities at the preceding grid line but has to be determined simultaneously with other unknowns along the same grid line. The relative advantage in this method is that there is no stability and convergence requirement. For brevity, the explicit, DuFort-Frankel explicit and implicit schemes will be referred to hereafter as the E, D-F and I schemes, respectively. These three schemes, which are most widely used, are to be discussed. The variants of these schemes as well as other methods will not be pursued here.

The finite-difference methods have been applied to viscous flow problems within the context of the boundary-layer theory by a number of investigators.[5-9]

Wu used the E scheme,[5] and Der and Raetz[7] employed the D-F scheme. Kramer and Lieberstein[6] and Flugge-Lotz and co-workers[8, 9] have applied and studied E and I schemes as well as their variants to a number of boundary-layer problems. None has studied and compared all three schemes. In addition, the singular behavior of the differential and difference equations of the present study differs from the singularities in the cited boundary-layer work because of the different formulations used. It is essential to observe in this connection that, in many boundary-layer works, the momentum-integral and other equivalent methods may be sufficient.[10] But for the present problem, as well as other hypersonic rarefied-gas flow problems, the integral methods (which also involve the stepwise numerical calculations) are shown to be inadequate because the velocity profiles do not permit simple description over a wide range of Reynolds number.

In the subsequent section, certain preliminary remarks on the errors, stability and convergence of the difference approximations will be given. The model of the flow problem and its governing equations are described in Section 3. In Section 4, essential details of the three finite difference methods are discussed. In Section 5, the results obtained with these methods are examined and the relative merit of the three schemes are evaluated.

II. STABILITY AND CONVERGENCE

In general, there are two types of errors which cause departures from the exact solution to the partial differential equation; truncation errors and round-off errors. The first arises from replacing the derivatives by the difference quotients and may be considered as an error resulting from the truncation of the Taylor series. The second results from the rounding-off in the numerical computation.* Generally, the effect of these errors may be controlled by reducing the spacing between grids and including more significant figures in the computation.

In practice, however, the departure from the exact solution due to each of these errors may grow or decay as computation progresses in a manner which is a property of the difference scheme.[2] Under certain circumstances, the rate of growth of the departure may become too large to be manageable, that is, it becomes unstable. On the other hand, there are schemes which are inherently stable in the sense that in the course of computation the departure due to errors tends to decay. Many schemes are only conditionally stable; the E scheme is one of the commonly known examples.[2,3] The D-F scheme is generally stable but subject to the problem of convergence. That is, as the spacing of the mesh is reduced, the solution of the difference equation can not always be reduced to that of the original differential equation.[2,3] The application of either of the E and D-F schemes is rather straightforward, but is handicapped by either the stability or convergence requirement which imposes restrictions on the choices

---

* Error may also result from the inaccurate description of the initial and boundary conditions.

of the increments in the two independent variables. In contrast, whereas the I scheme is generally free from both of the stability and convergence requirements.[2,3]

Apparently, in many cases, these restrictions can be satisfied by suitable adjustments to the spacing used for the mesh. However, for a differential equation such as the one to be considered, because of the singularity in the difference equation, the stability and convergence requirements may become stringent enough to make further refinements in the mesh size economically unfeasible. This singularity will occur at the apex of the cone, the leading edge of a flat plate or the stagnation region of a blunt body. In order to obtain the solution in the vicinity of the singularity, an expansion in ascending powers of the distance from the singular point has to be developed so that numerical integration may begin at some downstream station. In practice, this procedure introduces an error in the initial data because of the use of truncated series in the expansion. The error could, of course, be reduced by initiating the numerical integration at a station closer to the singularity, where higher-order terms in the expansion are not required. But, because of the singular behavior of the equations, moving the station upstream would reduce the scheme's accuracy as well as stability (if the scheme is only conditionally stable). Thus the presence of the singularity leads inevitably to the use of a refined mesh size in the vicinity of the singularity and to excessively long computation time.

III. THE FLOW MODEL AND ITS GOVERNING EQUATION

The flow model considered pertains to a continuum description of hypersonic, rarefied gas flows over cones. For simplicity, a perfect gas with constant specific heats is assumed. Without going through the details of the formulation based on the thin shock-layer theory of Cheng,[1] the differential equation governing the velocity under the assumption of a linear viscosity-temperature relation can be written for a cone or wedge in terms of a pair of dimensionless variables $\bar{x}$ and $\bar{\psi}$ as

$$\bar{x}\,\frac{\partial W}{\partial \bar{x}} = (1+\nu)\,\bar{\psi}\,\frac{\partial W}{\partial \bar{\psi}} + (1+\nu)^2\,\frac{\sqrt{2W}}{\bar{x}}\,\frac{\partial^2 W}{\partial \bar{\psi}^2} \tag{1}$$

The inner boundary condition, at $\bar{\psi} = 0$, is

$$W(0) = 0 \tag{2}$$

and the outer boundary condition immediately behind the shock, at $\bar{\psi} = 1$, is

$$\sqrt{2W} = 1 - \frac{(1+\nu)}{\bar{x}}\,\frac{\partial W}{\partial \bar{\psi}} \tag{3}$$

where $W \equiv \frac{1}{2}\left(\frac{u}{U_\infty \cos\beta}\right)^2$. U_∞ and u are the free-stream and local velocities respectively. The index ν is zero for a wedge and unity for a cone. For the present study, ν is therefore always taken as unity. The effects of the gas rarefaction as well as surface inclination are absorbed in the variable $\bar{x} \equiv \rho_\infty x/\mu_\infty U_\infty C \cos\beta = \varepsilon\, Re_x \sec\beta \left(\frac{\mu_0}{\mu_*}\cdot\frac{T_*}{T_0}\right)$ which is essentially a function of local Reynolds number. The variable $\bar{\psi}$ is related to the stream function ψ through $\bar{\psi} \equiv \psi / \rho_\infty U_\infty z (\pi z)^\nu$. One advantage of using $\bar{\psi}$ as an independent variable is that it eliminates the need for determining the location of the outer edge of the shock layer, as is evident from the boundary condition Eq. (3).

After the velocity is obtained, the total enthalpy can in turn be found. For a unit Prandtl number the Crocco relation gives[10,15]

$$H = H_w + (H_\infty - H_w)\frac{u}{U_\infty \cos\beta} \tag{4}$$

where subscripts ∞ and w denote the total enthalpies pertaining to free-stream and the surface conditions, respectively.

As is characteristic of the equations governing boundary layers and shock layers the coefficient of $\partial W/\partial x$ vanishes at $\bar{x} = 0$ which in this case is the cone apex. This will give rise to a singularity in any method employing forward integration in $\bar{x}$. In addition, because of the presence of $\sqrt{2W}\,(\sim\sqrt{\bar{\psi}})$, the equation and solution are also singular at the surface, i.e. $\bar{\psi} = 0$. The latter singularity can be avoided by using the combination of dependent and independent variables $\bar{u}$ and $(\bar{x}, \sqrt{\bar{\psi}})$, in place of W and $(\bar{x}, \bar{\psi})$. Subsequent discussion will show however that the singularity associated with $\bar{\psi} = 0$ turns out to be unimportant. In fact, corrections are not necessary for the present analysis.

As pointed out in the preceding discussion, a development in powers of $\bar{x}$ will be used to provide a solution in the vicinity of the apex and to furnish initial data for numerical integration beginning at some downstream station. The expansion admissible by the differential equations and boundary conditions, Eqs. (2) and (3), is of the form

$$W = W_0\,\bar{x} + W_1\,\bar{x}^{3/2} + W_2\,\bar{x}^2 + \cdots \tag{5}$$

or, alternatively

$$\bar{u} \equiv \frac{u}{U_\infty \cos\beta} = u_0\,\bar{x}^{1/2} + u_1\,\bar{x} + u_2\,\bar{x}^{3/2} + \cdots$$

where the coefficients u_0, u_1, etc. are determined after collecting equal powers of $\bar{x}$, as

$$
\left.
\begin{aligned}
u_0 &= \sqrt{\bar{\psi}} \\
u_1 &= -\frac{5}{12}\sqrt{\bar{\psi}} - \frac{1}{30}\,\bar{\psi}^{2} \\
u_2 &= \frac{1}{72}\left(\frac{187}{20}\sqrt{\bar{\psi}} - \bar{\psi}^{2} + \frac{11}{100}\,\bar{\psi}^{7/2}\right) \\
u_3 &= \frac{-1}{(12)^{3}\cdot 100}\left(3085\sqrt{\bar{\psi}} - 496\,\bar{\psi}^{2} - 105\,\bar{\psi}^{7/2} + \frac{16}{5}\,\bar{\psi}^{5}\right)
\end{aligned}
\right\} \quad (6)
$$

IV. THE THREE FINITE-DIFFERENCE METHODS

In the following, the resultant difference equation, in which the difference quotients approximate the partial derivatives, will be described for each of the three schemes mentioned. The manner in which the increments $\Delta\bar{x}$ and $\Delta\bar{y}$ will affect and control the errors, together with the stability and convergence characteristics of the schemes, will now be studied more closely. No attempt has been made to establish the proofs of stability and convergence for these schemes, which is clearly not the objective of this report; however, the stability and convergence for each of the schemes are demonstrated by the solutions obtained.

1. The Standard Explicit Scheme (E-Scheme)

(A) Difference Equation - For clarity, the reader is referred to the sketch of Fig. 1a. In this scheme, the data along a grid line, say m^{th} column, are assumed known; and the partial derivatives at a point in this column ($\bar{x}=m\Delta\bar{x}$, $\bar{y}=n\Delta\bar{y}$) are evaluated by the difference quotients which appear as the first terms in the following

$$\left.\begin{aligned}
\frac{\partial W}{\partial \bar{x}} &= \frac{W_{m+1,n}-W_{m,n}}{\Delta\bar{x}} - \frac{1}{2}(\Delta\bar{x})\,W_{\bar{x}\bar{x}} + \cdots\cdots \\
\frac{\partial W}{\partial \bar{y}} &= \frac{W_{m,n+1}-W_{m,n-1}}{2(\Delta\bar{y})} - \frac{1}{6}(\Delta\bar{y})^2\,W_{\bar{y}\bar{y}\bar{y}} + \cdots\cdots \\
\frac{\partial^2 W}{\partial \bar{y}^2} &= \frac{W_{m,n+1}-2W_{m,n}+W_{m,n-1}}{(\Delta\bar{y})^2} - \frac{1}{12}(\Delta\bar{y})^2 W_{\bar{y}\bar{y}\bar{y}\bar{y}} + \cdots\cdots
\end{aligned}\right\} \quad (7)$$

The second term on the right of each of the above equations represents the estimate of the truncation error based on Taylor's Theorem.

Upon using these difference quotients, Eq. (1) is approximately satisfied at the point (m , n) and the value of W at the downstream neighboring point $(m+1, n)$ can be evaluated explicitly in terms of values at the three points

$(m, n+1)$, (m, n) and $(m, n-1)$

$$W_{m+1,n} = W_{m,n} + \frac{\eta}{m}\left(W_{m,n+1} - W_{m,n-1}\right) + \frac{4\sqrt{2W_{m,n}}\,(\Delta\bar{z})}{\bar{z}^{\frac{1}{2}}(\Delta\bar{\psi})^{2}}\left(W_{m,n+1} - 2W_{m,n} + W_{m,n-1}\right) \qquad (8)$$

The boundary conditions in the finite-difference form will be discussed separately later, as they are applicable in the same manner to all three methods.

(B) Singularities and Truncation Error - Assuming that the solution W is regular in both $\bar{z}$ and $\bar{\psi}$, application of Eq. (7) introduces a truncation error in Eq. (8) belonging to the order of $\left[(\Delta\bar{z}) + (\Delta\bar{\psi})^{2}\right]$. When the step-sizes $\Delta\bar{z}$ and $\Delta\bar{\psi}$ are made successively smaller, one may anticipate that the truncation error will diminish and the solution to the difference equation Eq. (8) will converge to that of the differential equation Eq. (1). It is important to examine more carefully the nature of the truncation error in the neighborhood of $\bar{z} = 0$, as well as that of $\bar{\psi} = 0$ where the solution is singular.

The behavior of W near the cone surface, i.e. $\bar{\psi} = 0$, can be inferred from the differential equation Eq. (1) as

$$W = a\,\bar{\psi} + b\,\bar{\psi}^{5/2} + O\left(\bar{\psi}^{4}\right) \qquad (9)$$

where a and b are functions of $\bar{z}$. Because of the singular term $b\bar{\psi}^{5/2}$, the difference-quotient approximations of $W_{\bar{\psi}}$ and $W_{\bar{\psi}\bar{\psi}}$ will contain errors larger than the order of $(\Delta\bar{\psi})^{2}$ which, however, can be corrected. The largest errors of this kind occur at $\bar{\psi} = \Delta\bar{\psi}$, that is the first grid point from the boundary $\bar{\psi} = 0$. Using Eq. (9), one can express the difference quotients in terms of a and b. Thus, at $\bar{\psi} = \Delta\bar{\psi}$

$$\bar{W}_{\bar{\psi}} \equiv \frac{W(2\Delta\bar{\psi}) - W(0)}{2(\Delta\bar{\psi})} = a + b(2\sqrt{2})(\Delta\bar{\psi})^{3/2} + O(\Delta\bar{\psi})^{3}$$

$$\bar{W}_{\bar{\psi}\bar{\psi}} \equiv \frac{W(2\Delta\bar{\psi}) - 2W(\Delta\bar{\psi}) + W(0)}{(\Delta\bar{\psi})^{2}} = b(4\sqrt{2} - 2)(\Delta\bar{\psi})^{1/2} + O(\Delta\bar{\psi})^{2}$$

On the other hand, Eq. (9) also yields, at

$$W_{\bar\psi} = a + \frac{5}{2} b (\Delta\bar\psi)^{3/2} + O(\Delta\bar\psi)^3$$
$$W_{\bar\psi\bar\psi} = \frac{15}{4} b (\Delta\bar\psi)^{1/2} + O(\Delta\bar\psi)^2$$

It follows that, at the worst situation ($\bar\psi = \Delta\bar\psi$)

$$\left.\begin{aligned} \overline{W}_{\bar\psi} - W_{\bar\psi} &= b(2\sqrt{2} - \tfrac{5}{2})(\Delta\bar\psi)^{3/2} + O(\Delta\bar\psi)^3 \\ \overline{W}_{\bar\psi\bar\psi} - W_{\bar\psi\bar\psi} &= b(4\sqrt{2} - 2 - \tfrac{15}{4})(\Delta\bar\psi)^{1/2} + O(\Delta\bar\psi)^2 \end{aligned}\right\} \qquad (10)$$

The factors ($2\sqrt{2} - \frac{5}{2}$) and ($4\sqrt{2} - 2 - \frac{15}{4}$) have the values (+0.3284) and (−.0932), respectively. The magnitude of b is generally less than unity. In fact, the development given by Eq. (5) indicates that b is considerably less than 1/30. Therefore, having in mind an increment $\Delta\bar\psi$ of the order of 1/10, as in most of the present calculations, the truncation error resulting from the singularity at $\bar\psi = 0$ is numerically comparable to, or smaller than, $(\Delta\bar\psi)^2$. Consequently, correction of such an error is not necessary. Therefore, the function W will be treated as being regular with respect to all $\bar\psi$ for all three schemes.

The truncation error is affected more critically by the singularity at $\bar x = 0$ than that at $\bar\psi = 0$. In fact, it is so severely affected that the region near $\bar x = 0$ has to be excluded from the numerical integration. To elucidate how the truncation error depends on $\bar x$, one may apply Eq. (7) to the differential equation, Eq. (1), retaining the remainders of the difference quotients,

$$\overline{W}_{\bar x} - 2\frac{\bar\psi}{\bar x}\overline{W}_{\bar\psi} - \frac{4\sqrt{2W}}{\bar x^2}\overline{W}_{\bar\psi\bar\psi} = (\Delta\bar x)\frac{W_{\bar x\bar x}}{2} - (\Delta\bar\psi)^2\left(\frac{\bar\psi}{\bar x}\right)\frac{W_{\bar\psi\bar\psi\bar\psi}}{3} - \left(\frac{\Delta\bar\psi}{\bar x}\right)^2\frac{\sqrt{2W}}{6}W_{\bar\psi\bar\psi\bar\psi\bar\psi} \qquad (11)$$

where the functions $\overline{W}_{\bar x}$, $\overline{W}_{\bar\psi}$, and $\overline{W}_{\bar\psi\bar\psi}$ on the left-hand side are the difference quotients given in Eq. (7). The right-hand side of Eq. (11) represents the estimate of the truncation errors resulting from the difference approximation.

While $\bar{x}$ is seen to appear in the last two terms as $\frac{1}{\bar{x}}$ and $\frac{1}{\bar{x}^2}$ in Eq. (11), the manner in which these error terms will vary with $\bar{x}$ depend on the singular behavior of W with respect to $\bar{x}$. Applying the development of Eq. (5) for small $\bar{x}$, with the coefficients given by Eq. (6), the terms on the left-hand side of Eq. (11) are found to be the order of $\bar{\psi}$, whereas the three terms on the right-hand side in succession are, respectively, in the order of $(\Delta\bar{x})\bar{\psi}/\sqrt{\bar{x}}$, $(\Delta\bar{\psi})^2\sqrt{\bar{\psi}\cdot\bar{x}}$, and $(\Delta\bar{\psi})^2/\bar{\psi}$. The six terms in Eq. (11) are therefore in the proportion

$$O(1) : O(1) : O(1) : O\left[\frac{\Delta\bar{x}}{\sqrt{\bar{x}}}\right] : O\left[(\Delta\bar{\psi})^2\sqrt{\frac{\bar{x}}{\bar{\psi}}}\right] : O\left[\left(\frac{\Delta\psi}{\bar{\psi}}\right)^2\right] \qquad (12)$$

At a given $\bar{x}$, the last two terms of Eq. (12) become largest at the smallest value of $\bar{\psi}$; at $\bar{\psi} = \Delta\bar{\psi}$,* they become of the order $(\Delta\bar{\psi})^3\sqrt{\bar{x}}$ and 1, respectively. On account of the last of the remainders, the truncation error of the difference equation cannot be made arbitrarily small as $\Delta\bar{\psi}$ is made to vanish. Fortunately, the terms on the right-hand side of Eq. (11) associated with $\Delta\bar{\psi}$ are always small, numerically speaking. This fact can readily be checked by making use of the coefficients of Eq. (6). To represent more appropriately the relative magnitudes in a numerical sense, the last two terms in Eq. (12) have, in fact, to be multiplied by a factor of 1/30. Therefore, from a practical viewpoint, the finite-difference approximation may still be applicable for small $\bar{x}$.

(C) Stability - As pointed out before, the difficulty of the E scheme is not with the truncation error alone, rather, it is a problem of stability. For a

---

* The difference equation is not applied at $\bar{\psi} = 0$.

simple parabolic equation, e. g.

$$\frac{\partial u}{\partial x} = \sigma \frac{\partial^2 u}{\partial y^2} \tag{13}$$

with a constant coefficient σ , the criterion for the stability of the E scheme is[3]

$$2\sigma \frac{\Delta x}{(\Delta y)^2} \leq 1 \tag{14}$$

The presence of a lower-order derivative, such as $\frac{\partial u}{\partial y}$, and u will affect the stability characteristics of the difference equation only through terms of orders higher than Δx and $(\Delta y)^2$; consequently they are not important from a practical viewpoint. Similarly, the presence of variable coefficients,[2, 3] as well as the nonlinearity, may also be looked upon as higher-order effects in the stability consideration, provided that the coefficient σ be interpreted locally, and that increments Δx and Δy be taken sufficiently small.

It should be noted at this point that Eq. (14) can be shown to be the necessary and sufficient condition for the stability of the E-scheme with a constant coefficient σ (see Refs. 11 and 12). It has also been shown that Eq. (14) is a sufficient condition for stability of the E-scheme for a quasi-linear equation[13]

$$\frac{\partial u}{\partial x} = a_0(x,y)\frac{\partial^2 u}{\partial y^2} + a_1(x,y)\frac{\partial u}{\partial y} + a_2(x,y)u$$

In this connection, a criterion based on an electric network analogy may be of interest. By considering the stability for the current or voltage in an electric network, Karplus[14] studies the difference equation in the form

$$\left.\begin{aligned}(W_{m+1,n}-W_{m,n})+a(W_{m-1,n}-W_{m,n})+b(W_{m+2,n}-W_{m,n})\\ +c(W_{m-2,n}-W_{m,n})+\text{----------}\\ +d(W_{m,n+1}-W_{m,n})+e(W_{m,n-1}-W_{m,n})\\ +\text{----------}\qquad\qquad =0\end{aligned}\right\} \tag{15}$$

where a, b, c, d, and e are the coefficients of the difference terms. It has been shown in Ref. 14 that if all the coefficients are positive, the equation is stable; and if some of the coefficients are negative, a sufficient condition for stability is that the algebraic sum of all the coefficients be negative. For the simple parabolic equation, Eq. (13), application of the Karplus condition to the E-scheme yields the criterion of Eq. (14). The Karplus condition may be quite useful in suggesting stability characteristics of new schemes.

For the stability of Eq. (8) of the E scheme the criterion Eq. (14) gives the condition

$$\frac{8\sqrt{2W}\,(\Delta\bar{x})}{\bar{x}^{2}(\Delta\bar{\psi})^{2}} < 1 \tag{16}$$

The factor $1/\bar{x}^{2}$ in the above inequality places such a stringent restriction on step sizes that either the increments in $\bar{x}$ become, time wise, intolerably small or the increments in $\bar{\psi}$ becomes too large for acceptable truncation errors.

2. The Explicit Scheme of DuFort and Frankel (D-F Scheme)

(A) Difference Equation - Referring to the sketch (b) of Figure 1, for the D-F scheme, the unknown quantity at a grid point ($m+1$, n) is evaluated in terms of the known quantities at the points (m, $n+1$), (m, $n-1$) and ($m-1$, n). Determination of the value at the new

point ($m+1, n$) therefore involves data along two preceding grid lines, i.e. the m-th and ($m-1$) th columns. The difference quotients for the D-F scheme are the first terms in the following developments[2, 3, 4]

$$\left.\begin{aligned}
\frac{\partial W}{\partial \bar{x}} &= \frac{W_{m+1,n} - W_{m-1,n}}{2(\Delta \bar{x})} - \frac{1}{6}(\Delta \bar{x})^2 W_{\bar{x}\bar{x}\bar{x}} + \cdots\cdots\cdots \\
\frac{\partial W}{\partial \bar{\psi}} &= \frac{W_{m,n+1} - W_{m,n-1}}{2(\Delta \bar{\psi})} - \frac{1}{6}(\Delta \bar{\psi})^2 W_{\bar{\psi}\bar{\psi}\bar{\psi}} + \cdots\cdots\cdots \\
\frac{\partial^2 W}{\partial \bar{\psi}^2} &= \frac{W_{m,n+1} - 2W_{m,n} + W_{m,n-1}}{(\Delta \bar{\psi})^2} - \frac{1}{12}(\Delta \bar{\psi})^2 W_{\bar{\psi}\bar{\psi}\bar{\psi}\bar{\psi}} + \cdots\cdots\cdots \\
&= \frac{W_{m,n+1} - W_{m+1,n} - W_{m-1,n} + W_{m,n-1}}{(\Delta \bar{\psi})^2} + \left(\frac{\Delta \bar{x}}{\Delta \bar{\psi}}\right)^2 W_{\bar{x}\bar{x}} - \frac{(\Delta \bar{\psi})^2}{12} W_{\bar{\psi}\bar{\psi}\bar{\psi}\bar{\psi}} + \cdots\cdots
\end{aligned}\right\} \quad (17)$$

The difference quotients used in the D-F scheme, which do not involve the point (m, n) differ from those of Eq. (7) in the E scheme. With Eq. (17) the differential Eq. (1) can be satisfied approximately at the point (m, n). The following difference equation is obtained

$$W_{m+1,n} = \frac{1}{A_1} \cdot \left(A_2 W_{m-1,n} + A_3 W_{m,n+1} + A_4 W_{m,n-1} \right) \quad (18)$$

where

$$A_1 = 1 + \frac{8\sqrt{2W_{m,n}}(\Delta \bar{x})}{\bar{x}^2 (\Delta \bar{\psi})^2}, \qquad A_3 = \frac{8\sqrt{2W_{m,n}}(\Delta \bar{x})}{\bar{x}^2 (\Delta \bar{\psi})^2} + 2\frac{n}{m}$$

$$A_2 = 1 - \frac{8\sqrt{2W_{m,n}}(\Delta \bar{x})}{\bar{x}^2 (\Delta \bar{\psi})^2}, \qquad A_4 = \frac{8\sqrt{2W_{m,n}}(\Delta \bar{x})}{\bar{x}^2 (\Delta \bar{\psi})^2} - 2\frac{n}{m}$$

In order to determine W at the unknown point ($m+1, n$), values of W at four points of preceding grid lines ($m, n+1$), (m, n), ($m, n-1$) and ($m-1, n$) have to be used. It may be noted that if the coefficients in the differential equation were constants, the information at the point (m, n) would not be required, since the difference quotients of this scheme do not

involve the point (m, n).

The above difference Equation (18) is stable for all values of $(\Delta\bar{x})$ and $(\Delta\bar{\psi})$, and the results to be cited here corroborate this conclusion. Some further discussion on the stability of the D-F scheme for the case of constant coefficient has been described by Forsythe[2] and by Richtmeyer.[3]

(B) Truncation Error and Convergence

Assuming that W is regular, the difference equation Eq. (18) is subject to a truncation error of $O[(\Delta\bar{x})^2+(\Delta\bar{\psi})^2+(\Delta\bar{x}/\Delta\bar{\psi})^2]$. The term $O(\Delta\bar{x}/\Delta\bar{\psi})^2$, which results from the remainder $(\Delta\bar{x}/\Delta\bar{\psi})^2 W_{\bar{x}\bar{x}}$ in the second-order difference quotient of Eq. (17), reveals an undesirable feature of the D-F scheme. That is, the truncation error introduced by the difference quotients cannot be reduced by considering arbitrarily small $\Delta\bar{x}$ and $\Delta\bar{\psi}$ alone, but rather it is necessary to impose the condition $\Delta\bar{x} \ll \Delta\bar{\psi} \ll 1$; otherwise, the difference equation will not converge to the parabolic equation, but to one of a hyperbolic type.

In order to estimate the magnitudes of the truncation error contributed by various terms of a difference equation similar to that of Eq. (11) may be written to include the remainders of Eq. (17) in the following form

$$\left.\begin{aligned} \overline{W}_{\bar{x}} - 2\frac{\bar{\psi}}{\bar{x}}\overline{W}_{\bar{\psi}} - 4\frac{\sqrt{2W}}{\bar{x}^2}\overline{W}_{\bar{\psi}\bar{\psi}} = {} & (\Delta\bar{x})^2\frac{W_{\bar{x}\bar{x}\bar{x}}}{6} - (\Delta\bar{\psi})^2\frac{\bar{\psi}}{\bar{x}}\cdot\frac{W_{\bar{x}\bar{\psi}\bar{\psi}}}{3} \\ & - \frac{(\Delta\bar{\psi})^2}{\bar{x}^2}\cdot\frac{\sqrt{2W}}{6}W_{\bar{\psi}\bar{\psi}\bar{\psi}\bar{\psi}} + \left(\frac{\Delta\bar{x}}{\Delta\bar{\psi}}\right)^2\frac{4\sqrt{2W}}{\bar{x}^2}\cdot W_{\bar{x}\bar{x}} \end{aligned}\right\} \quad (19)$$

where $\overline{W}_{\bar{x}}$, $\overline{W}_{\bar{\psi}}$ and $\overline{W}_{\bar{\psi}\bar{\psi}}$ are the difference quotients which in this case are those defined by the first terms of Eq. (17). The terms on the right-hand side of Eq. (19) constitute the truncation error of the difference equation

Eq. (18). As $\bar{x} \longrightarrow 0$, and with the aid of Eq. (5) the seven terms of Eq. (19) can be shown to be in the proportion

$$O(1):O(1):O(1):O\left[\frac{(\Delta\bar{x})^2}{\bar{x}^{1/2}}\right]:O\left[(\Delta\bar{\psi})^2\sqrt{\frac{\bar{x}}{\bar{\psi}}}\right]:O\left[\left(\frac{\Delta\bar{\psi}}{\bar{\psi}}\right)^2\right]:O\left[\left(\frac{\Delta\bar{x}}{\Delta\bar{\psi}}\right)^2\frac{\sqrt{\bar{\psi}}}{\bar{x}^2}\right] \qquad (20)$$

Clearly, the presence of the singularity at $\bar{x} = 0$ not only magnified the truncation error in the D-F scheme but also makes the problem of convergence more critical.*

3. Implicit Scheme (I Scheme)

(A) Difference Equation

In this scheme, the unknown quantities along a column of grid points, say the $(m+1)$-column, are solved simultaneously with known data along the m th grid line (refer to sketch (c) of Fig. 1). The difference quotients defining the I-scheme are constructed according to the first terms in the following expansion[2,9]

$$\left.\begin{aligned}
\frac{\partial W}{\partial \bar{x}} &= \frac{W_{m+1,n} - W_{m,n}}{(\Delta\bar{x})} - \frac{1}{2}(\Delta\bar{x})W_{\bar{x}\bar{x}} + \cdots\cdots\cdots \\
\frac{\partial W}{\partial \bar{\psi}} &= \frac{W_{m+1,n+1} - W_{m+1,n-1}}{2(\Delta\bar{\psi})} - \frac{1}{6}(\Delta\bar{\psi})^2 W_{\bar{\psi}\bar{\psi}\bar{\psi}} + \cdots\cdots\cdots \\
\frac{\partial^2 W}{\partial \bar{\psi}^2} &= \frac{W_{m+1,n+1} - 2W_{m+1,n} + W_{m+1,n-1}}{(\Delta\bar{\psi})^2} - \frac{(\Delta\bar{\psi})^2}{12} W_{\bar{\psi}\bar{\psi}\bar{\psi}\bar{\psi}} + \cdots\cdots
\end{aligned}\right\} \qquad (21)$$

With the difference quotients of Eq. (21), the differential equation, Eq. (1), is reduced to a system of linear algebraic equations with the W's in the $(m+1)$-column.

---

*For numerical consideration, one must multiply the fifth and the sixth terms in Eq. (20) by a factor of 1/30. Note also that $\bar{\psi} \geq \Delta\bar{\psi}$

$$f(n)W_{m+1,n-1} + g(n)W_{m+1,n} + h(n)W_{m+1,n-1} = W_{m,n} \qquad (22)$$

where

$$f(n) = \frac{n}{m} - \frac{4\sqrt{2W_{m,n}}\,(\Delta\bar{x})}{\bar{x}^2(\Delta\bar{\psi})^2}$$

$$g(n) = 1 + \frac{8\sqrt{2W_{m,n}}\,(\Delta\bar{x})}{\bar{x}^2(\Delta\bar{\psi})^2}$$

$$h(n) = -\left(\frac{n}{m}\right) - \frac{4\sqrt{2W_{m,n}}\,(\Delta\bar{x})}{\bar{x}^2(\Delta\bar{\psi})^2}$$

The integer n is taken from 1 to N for each m, with $n = 1$ corresponding to the first grid point from the "cone surface" and $n = N$ corresponding to the boundary point at the shock. Or, in an expansion form

$$\left.\begin{aligned}
f(1)W_{m+1,0} + g(1)W_{m+1,1} + h(1)W_{m+1,2} &= W_{m,1} \\
f(2)W_{m+1,1} + g(2)W_{m+1,2} + h(2)W_{m+1,3} &= W_{m,2} \\
f(3)W_{m+1,2} + g(3)W_{m+1,3} + h(3)W_{m+1,4} &= W_{m,3} \\
&\cdots\cdots \\
f(N-1)W_{m+1,N-2} + g(N-1)W_{m+1,N-1} + h(N-1)W_{m+1,N} &= W_{m,N-1}
\end{aligned}\right\}$$

where $W_{m+1,0}$ and $W_{m+1,N}$ denote values to be determined by the inner and outer boundary conditions respectively. These equations, together with the two boundary conditions, form a system which suffices for the determination of the ($N+1$) unknowns. The matrix of this system is of the tridiagonal type, and the solution can thus be obtained by following standard procedures,

e.g. Gauss' elimination method.[2]

(B) Truncation Error

The choice of the mesh spacings for $\Delta\bar{x}$ and $\Delta\bar{\psi}$ in this scheme is not subject to the stability and the convergence requirements.[2,3] Generally, in the I-scheme, the difference equation, Eq. (22), is subject to the truncation errors of the order $[(\Delta\bar{x})+(\Delta\bar{\psi})^2]$. The error of $O(\Delta\bar{x})$ arises from the use of the backward-difference quotient for $\partial W/\partial\bar{x}$ as well as from replacing $\sqrt{2W_{m+1,n}}$ by $\sqrt{2W_{m,n}}$. Note that the differential equation is satisfied in this scheme at the station $(m+1)$. To examine more thoroughly the manner by which the singularity at $\bar{x}=0$ affects the truncation error, one may again express the difference equations, Eq. (22), in a form similar to that of Eq. (11) and (19).

$$\left.\begin{aligned}\overline{W}_{\bar{x}}-2\frac{\bar{\psi}}{\bar{x}}\overline{W}_{\bar{\psi}}-4\frac{\sqrt{2W}}{\bar{x}^2}\overline{W}_{\bar{\psi}\bar{\psi}} &= (\Delta\bar{x})\frac{W_{\bar{x}\bar{x}}}{2}-(\Delta\bar{\psi})^2\frac{\bar{\psi}}{\bar{x}}\frac{W_{\bar{\psi}\bar{\psi}\bar{\psi}}}{3}\\ &\quad-\frac{(\Delta\bar{\psi})^2}{\bar{x}^2}\frac{\sqrt{2W}}{3}W_{\bar{\psi}\bar{\psi}\bar{\psi}\bar{\psi}}+\frac{\Delta\bar{x}}{\bar{x}^2}\frac{2}{\sqrt{2W}}W_{\bar{x}}W_{\bar{\psi}\bar{\psi}}\end{aligned}\right\} \qquad (23)$$

where the terms on the right-hand side again represent the remainder of the difference equation. The same estimate of each term in Eq. (11) holds for the corresponding term in Eq. (23) except the last (additional) term, which arises from replacing $\sqrt{2W_{m+1,n}}$ by $\sqrt{2W_{m,n}}$, is of the order of $(\Delta\bar{x}/\bar{x})\cdot\bar{\psi}$. As $\bar{x}\longrightarrow 0$, the seven terms of Eq. (23) are thus in the proportion

$$O(1):O(1):O(1):O\left[\frac{\Delta\bar{x}}{\sqrt{\bar{x}}}\right]:O\left[(\Delta\bar{\psi})^2\sqrt{\frac{\bar{x}}{\bar{\psi}}}\right]:O\left[\left(\frac{\Delta\bar{\psi}}{\bar{\psi}}\right)^2\right]:O\left[\frac{\Delta\bar{x}}{\bar{x}}\right] \qquad (24)$$

Clearly the accuracy of this scheme is still greatly affected by the singular point. The problem, however, is far less critical than encountered in the E

and D-F schemes.*

4. Boundary Conditions

The conditions at the "cone surface" and at the shock are the inner and outer boundary conditions, respectively. The difference equation for the inner boundary condition is simply

$$W_{m+1,0} = 0 \tag{25}$$

In order to determine W at the outer boundary with an accuracy comparable to that obtained with the difference equations, the derivative $\partial W/\partial \bar{\psi}$ at a boundary point will be expressed in terms of W at the neighboring points (refer to sketch (d) in Fig. 1) as

$$\left.\frac{\partial W}{\partial \bar{\psi}}\right|_{m+1,N} = \frac{3W_{m+1,N} - 4W_{m+1,N-1} + W_{m+1,N-2}}{2(\Delta\bar{\psi})^2} + O(\Delta\bar{\psi})^2 \tag{26}$$

Notice that, because of the term $\sqrt{2W}$, the boundary condition Eq. (3) is nonlinear. Hence, one would have to solve a quadratic algebraic equation for the boundary value of W. To simplify the numerical computation, one may replace $\sqrt{2W_{m+1,N}}$ by $\sqrt{2W_{m,N}}$, which introduces only an error of $O(\Delta\bar{x})$ and is consistent with the accuracy of all three schemes. The outer boundary conditions can therefore be satisfied

$$W_{m+1,N} = \frac{4}{3}W_{m+1,N-1} - \frac{1}{3}W_{m+1,N-2} + \bar{x}(\Delta\bar{\psi})\frac{1}{3}\left(1 - \sqrt{2W_{m,N}}\right) \tag{27}$$

In the implicit scheme, Eq. (27) is used to eliminate $W_{m+1,N}$ in the last equation of the system of Eq. (22).

---

* Again, in order to compare the relative magnitudes of the terms in Eq. (24) in a strict numerical sense, one must multiply both $(\Delta\bar{\psi})^2\sqrt{\bar{x}/\bar{\psi}}$ and $(\Delta\bar{\psi}/\bar{\psi})^2$ by a factor of 1/30.

V. DISCUSSION OF RESULTS

In the preceding sections, three difference schemes have been described for the cone problem. Excluding the region near the singularity $\bar{x} = 0$, the truncation error in the difference approximation belongs to $O[(\Delta\bar{x})+(\Delta\bar{\psi})^2]$ for the E and I schemes, and to $O\left[(\Delta\bar{\psi})^2+\left(\frac{\Delta\bar{x}}{\Delta\bar{\psi}}\right)^2\right]$ for the D-F scheme. By making $\Delta\bar{x} \ll \Delta\bar{\psi} \ll 1$, not only can the truncation errors in all the schemes be reduced, but also the stability and convergence requirements for the E and D-F schemes can be satisfied.

The singularity at $\bar{x} = 0$ makes the accuracy of the solution, or alternatively the efficiency of all three schemes, very poor, as the cone apex is approached. The singularity also makes the stability and convergence problems of the E and D-F schemes more critical. This poses a serious problem in practice, because application of any of these schemes over a range of $\bar{x}$, which begins at a large $\bar{x}$ to avoid the adverse effect of the singularity, cannot avoid encountering a difficulty of another kind. For, in order to provide accurate initial data at a station far removed from $\bar{x} = 0$, one has to use a large number of high-order terms in the development of Eq. (5). In Eq. (5), a four-term expansion has been obtained for the purpose of the present study. But in other more general problems, the task of determining the coefficients of the higher-order terms would be too burdensome.

In the following comparison of the three schemes, examination will be made first over the range $0.2 \leq \bar{x} \leq 1$, and then over a more critical range $.01 \leq \bar{x} \leq 0.2$. The skin-friction and heat-transfer coefficients, as well as the velocity profiles obtained by the I-scheme will be presented over a wide range: $0.01 \leq \bar{x} \leq 10$.

5.1 Numerical Integration Beginning at $\bar{x} = 0.20$

From the Crocco relation Eq. (4),

$$C_H = C_F / 2 \cos\beta \tag{28}$$

where C_H and C_F are the surface heat-transfer and skin-friction coefficients, defined as

$$\left.\begin{aligned} C_H &\equiv \frac{\left(k \frac{\partial T}{\partial y}\right)_w}{\rho_\infty U_\infty (H_\infty - H_w)} = \frac{1}{\bar{x}} \frac{\partial W}{\partial \bar{\psi}} \sin\beta \\ C_F &\equiv \frac{\left(\mu \frac{\partial u}{\partial y}\right)_w}{\frac{1}{2} \rho_\infty U_\infty^2} = \frac{1}{\bar{x}} \frac{\partial W}{\partial \bar{\psi}} \sin 2\beta \end{aligned}\right\} \tag{29}$$

Typical results obtained from the three methods are presented in Figs. 2 and 3. In Fig. 2, C_H and C_F obtained by the E, I and D-F schemes over the range $0.2 \leq \bar{x} \leq 1.0$ are compared. In order to provide the initial data at $\bar{x} = 0.2$ with an error no more than 1%, all terms in the four-term expansion in $\bar{x}$ given in Eq. (5) have to be used. The calculations were performed by an IBM 704 digital computer, carrying eight significant figures.

It was found that the choice of $\Delta\bar{\psi} = 1/10$ is sufficient for all three schemes. However, the step-size $\Delta\bar{x}$ had to be varied with different schemes to accomodate the stability and convergence requirements as well as the singularity affect on truncation errors. In the E scheme, the increment $\Delta\bar{x} < 5 \times 10^{-5}$ is required in order to fulfill the stability condition at $\bar{x} = .20$. A smaller step-size $\Delta\bar{x} = 2.5 \times 10^{-5}$ was chosen in the calculation because instability has actually occurred with $\Delta\bar{x} = 5 \times 10^{-5}$. Two runs were made for each of the I and D-F schemes, first with $\Delta\bar{x} = 1/100$, $\Delta\bar{\psi} = 1/10$ and the second with $\Delta\bar{x} = 1/1000$, $\Delta\bar{\psi} = 1/10$. The good agreement among results of the second runs of I and D-F schemes as well as the E scheme provides a preliminary indication of the adequate accuracy of these schemes. The accuracies

are less satisfactory for the first runs of the I and D-F schemes with $\Delta\bar{\chi} = 1/100$, particularly the latter. The total computation times (including print-out at the .05-intervals of $\bar{\chi}$) are approximately 45 minutes for the E scheme, 20 seconds for the first runs of the I and D-F schemes, and 100 seconds for the second runs of the I and D-F schemes.

Notice that the running time for both I and D-F schemes are about the same; nevertheless, with the same set of increments, the D-F scheme is less accurate as shown in Fig. 2.

5.2 Numerical Integration Beginning at $\bar{\chi} = .01$

As a more crucial test of the usefulness of the methods, calculations were carried out and compared over the range of a smaller $\bar{\chi}$ ($0.1 \leq \bar{\chi} \leq 0.3$). The initial data can be adequately provided by the first two-terms in the development of Eq. (5) but the problems of the singularity tends to be more critical. In fact, the computation by IBM 704 for the E scheme becomes virtually impossible under the stringent stability requirement over this range. Thus, only the results from I and D-F schemes are considered. The two schemes are first carried out with the increments $\Delta\bar{\chi} = 1/100$, and $\Delta\bar{\psi} = 1/10$, then with $\Delta\bar{\chi} = 1/1000$ and $\Delta\bar{\psi} = 1/10$. As shown in Fig. 3, the departure of the solution by the D-F scheme is greatly amplified at small $\bar{\chi}$, where the singularity makes satisfaction of the convergence requirement more difficult. Even in the second run with a more refined step-size in $\bar{\chi}$, a small but appreciable error of about 4% still exists for the D-F scheme. The I-scheme in the second run with $\Delta\bar{\chi} = 1/1000$ and $\Delta\bar{\psi} = 1/10$ yields good accuracy, agreeing with the four-term analytic development of Eq. (5) throughout the entire range of $.01 \leq \bar{\chi} \leq .3$. The computation time

(including print-out) of the runs with $\Delta\bar{x} = 1/1000$ and $\Delta\bar{\psi} = 1/10$ was about 110 seconds for each scheme.

5.3 Discussion on the Efficiency of the Three Schemes

In summarizing the results presented in Figs. 2 and 3, the E scheme is definitely less efficient and not suitable for the treatment of singular differential equations such as Eq. (1). With the same intervals of $\Delta\bar{x}$ and $\Delta\bar{\psi}$, the computation time for the E scheme is 45 minutes, but only 20 seconds for the I and D-F schemes. The examples show that the singularity at $\bar{x} = 0$ affects critically the accuracy and efficiency of both the I and the D-F schemes, especially if higher-order terms in the development about the singular point are not available. The I scheme, which is subject to neither the stability nor the convergence requirements, proves in this instance to be somewhat more reliable than the D-F scheme. This relative merit of the I scheme is comprehensible in the light of the discussion in Section IV. One may recall that the largest truncation error in the I scheme is of $O(\frac{\Delta\bar{x}}{\bar{x}})$ whereas the largest in the D-F scheme is of $O\left[\left(\frac{\Delta\bar{x}}{\Delta\bar{\psi}}\right)^2 \frac{\sqrt{\bar{\psi}}}{\bar{x}^2}\right]$.

It is of interest to note that the truncation errors associated with $\Delta\bar{\psi}$ were found to be very small. Calculations have been repeated with $\Delta\bar{\psi}$ changed from 1/10 to 1/50 without appreciable difference in the solution. The comparative insensitivity of the solutions to the interval $\Delta\bar{\psi}$ in both the I and D-F schemes is also understandable from the previous discussion, that there is always a small numerical factor associated with the $(\Delta\bar{\psi})^2$ terms in the remainders of the difference equation, which compensates partly for the adverse effects of the singularity. This insensitivity is, of course, a property peculiar to the specific problem considered. However,

in a more general case, especially if the pressure gradients do not vanish, one may have to refine not only the increment in $\bar{x}$ but also the step-size of $\Delta\bar{\psi}$ as $\bar{x} \longrightarrow 0$.* In that case, the freedom from the convergence requirement makes the I scheme even more superior.

5.4 Discussion of the Numerical Solutions

In order to demonstrate the accuracy of the method the numerical solution to Eqs. (1) - (3) is carried out for hypersonic flow over a cone under the I scheme from $\bar{x} = 0.01$ to $\bar{x} = 10$. The computation was made in two stages of different step sizes in $\bar{x}$. In the first stage, the integration by the I scheme, with $\Delta\bar{x} = 1/1000$, $\Delta\bar{\psi} = 1/10$, was carried out from $\bar{x} = 0.01$ to $\bar{x} = 0.2$ with the initial data provided by the four-term expansion of Eq. (5). The integration by I scheme was continued in the second stage from $\bar{x} = 0.2$ through 10 with a larger step-size in $\bar{x}$, ($\Delta\bar{x} = 1/100$, $\Delta\bar{\psi} = 1/10$). The total computation time (including print-out at 0.05 interval of $\bar{x}$) was about two minutes, with 38 seconds for the first stage and 90 seconds for the second stage. The results for skin friction, surface heat-transfer rate, and velocity profiles are presented in Figs. 4, 5, and 6.

The ratios of $C_H/\sin\beta$ and $C_F/\sin 2\beta$ given in Fig. 4 are in good agreement with the analytic development obtained for the region of $\bar{x} < 1$, and approach the correct values of the classical boundary-layer theory for $\bar{x} \longrightarrow \infty$. The velocity profiles of the shock layer at various distances from the apex are given in Fig. 5. At low value of $\bar{x}$, the distribution is

*In such a general case, the correction for the singularity associated with $\bar{\psi} = 0$ will be no longer as small as represented by Eq. (10), and cannot be neglected. However, as pointed out previously, this singularity can be eliminated by using the variable $\bar{u}$ and $\sqrt{\bar{\psi}}$ instead of W and $\bar{\psi}$. The new variables will introduce a factor of $1/\sqrt{\bar{\psi}}$ to the remainder of the difference equations and make the use of the I scheme (rather than other schemes) more desirable.

linear in $\sqrt{\bar{\psi}}$ corresponding to a uniform shear flow. As $\bar{\chi}$ increases, the velocity gradient increases near the surface and decreases near the shock, with the velocity in the outer portion approaching to the tangential component of the free-stream velocity.

It is rather interesting to observe that, even at $\bar{\chi}$ as low as 3, the flow field can already be represented very closely by the classical boundary-layer limit, in spite of the fact that the velocity at the outer edge is still quite far from the inviscid value and that the viscous layer is still a major fraction of the shock layer. To clearly demonstrate this observation, the velocity profiles at various $\bar{\chi}$ stations are correlated in terms of the similarity variable

$$\eta \equiv \sqrt{\frac{3\bar{\chi}}{3+\bar{\psi}}} \int_0^{\bar{\psi}} \frac{d\bar{\psi}}{\sqrt{2W}} \tag{30}$$

and presented in Fig. 6. The good correlation and excellent agreement with the Blasius profile provide another check on the validity and accuracy of the method.

It should be noted that, in order to apply the solution obtained, one must relate the variable $\bar{\chi}$ with the Reynolds number (or its reciprocal, the Knudsen number) based on the free-stream flow condition. This involves a choice of the reference temperature T_* because of the linear viscosity-temperature relation used,[1,15] which in this case may be simply taken as

$$\frac{T_*}{T_0} = \frac{1}{\bar{u}(1)} \int_0^{\bar{u}(1)} \frac{T}{T_0} d\bar{u} = \frac{T_w}{T_0} + \left(1 - \frac{T_w}{T_0}\right) \frac{\bar{u}(1)}{2} - \cos^2\beta \frac{[\bar{u}(1)]^2}{3}$$

VI. CONCLUSION

The relative merit of three difference schemes for integrating the viscous shock-layer equation has been investigated with specific reference to the problem of low density hypersonic flow over a cone. The difference quotients and equations defining each of the schemes have been derived and the nature of the singularities on the solution and their effects on the stability and convergence characteristics of these schemes were studied.

There are two singularities in the solution. One is associated with the leading-edge ($\bar{x} = 0$) and the other with the cone surface ($\psi = 0$). Close examination shows that the latter has little effect on the results. The leading-edge singularity on the other hand critically affects the accuracy and efficiency of all schemes, particularly the stability characteristics of the explicit scheme. Because of this effect, one must either increase the number of the higher-order terms in the power-series expansion around the leading edge (so as to maintain the accuracy of the initial data at a comparatively large value of $\bar{x}$), or further refine the step-size in $\bar{x}$ (so as to maintain the accuracy of the difference equation at a comparatively small value of $\bar{x}$).

The three schemes applied to the cone problem were carried out with the aid of the IBM 704 digital computer. The results indicate that, because of the leading-edge singularity, the stability requirement becomes too stringent for the explicit scheme to be useful. While the difference in efficiency of the implicit and DuFort-Frankel schemes is actually not large for this example, the implicit scheme, which is subject to neither the stability nor the convergence requirements, is seen to be more reliable. It is noted, furthermore, that in the more general problems with non-vanishing pressure gradients, the implicit scheme should be more advantageous.

REFERENCES

1. Cheng, H. K., Hypersonic Shock-Layer Theory of the Stagnation Region at Low Reynolds Number. Proc. Heat Transfer & Fluid Mech. Inst., p. 161, Univ. So. Calif., Stanford Univ. Press, June 1961.

2. Forsythe, G. E. and Wasow, W. R., Finite-Difference Methods for Partial Differential Equations. Wiley, 1960.

3. Richtmeyer, R. D., Difference Methods for Initial-Value Problems. Interscience Publishers, Inc., 1957.

4. DuFort, E. C. and Frankel, S., Stability Conditions in the Numerical Treatment of Parabolic Differential Equations. Math. Tables and Other Aids to Computations, Vol. VII, No. 43, July 1953.

5. Wu, J. C., On the Finite Difference Solution of Laminar Boundary-Layer Problems. Paper presented at Proc. Heat Transfer & Fluid Mechanics Institute, p. 55, Univ. So. Calif., June 1960.

6. Kramer, R. F. and Leiberstein, H. M., Numerical Solution of Boundary Layer Equations Without Similarity Assumptions. J. Aero. Sci. 26, 8, 1959.

7. Der, J. and Raetz, G. S., Solution of General Three-Dimensional Laminar Boundary-Layer Problems by an Exact Numerical Method. Paper presented at IAS 30th Annual Meeting, January 1962.

8. Flugge-Lotz, I. and Yu, E. Y., Development of a Finite-Difference Method for Computing a Compressible Laminar Boundary Layer with Interaction. Division of Engineering Mechanics, Stanford Univ. Tech. Rept. No. 127 (AFOSR TN 60-577), May 5, 1960.

9. Flugge-Lotz, I. and Blottner, F. G., Computation of the Compressible Laminar Boundary-Layer Flow Including Displacement Thickness Interaction Using Finite-Difference Methods. Division of Engineering Mech., Stanford Univ. Tech. Rept. No. 131 (AFOSR 2206), January 1962.

10. Schlichting, H., Boundary Layer Theory. McGraw-Hill, New York, 1955.

11. Hildebrand, F. B ., Methods of Applied Mathematics. Prentice Hall, 1952.

12. O'Brien, G. G., Hyman, M. S. and Kaplan, S., A Study of the Numerical Solution of Partial Differential Equations. Jour. of Math & Phys., Cambridge, Mass., Vol. 29, No. 4, pp. 223-251, January 1952.

13. John, F., On the Integration of Parabolic Equations by Difference Methods. Communications Pure & Appl. Math., Vol. 5, p. 155, 1952.

14. Karplus, W. J., An Electric Circuit Theory Approach to Finite-Difference Stability. AIEE, 77, 1, 1958.

15. Hayes, W. D. and Probstein, R., Hypersonic Flow Theory. Academic Press, New York, 1959.

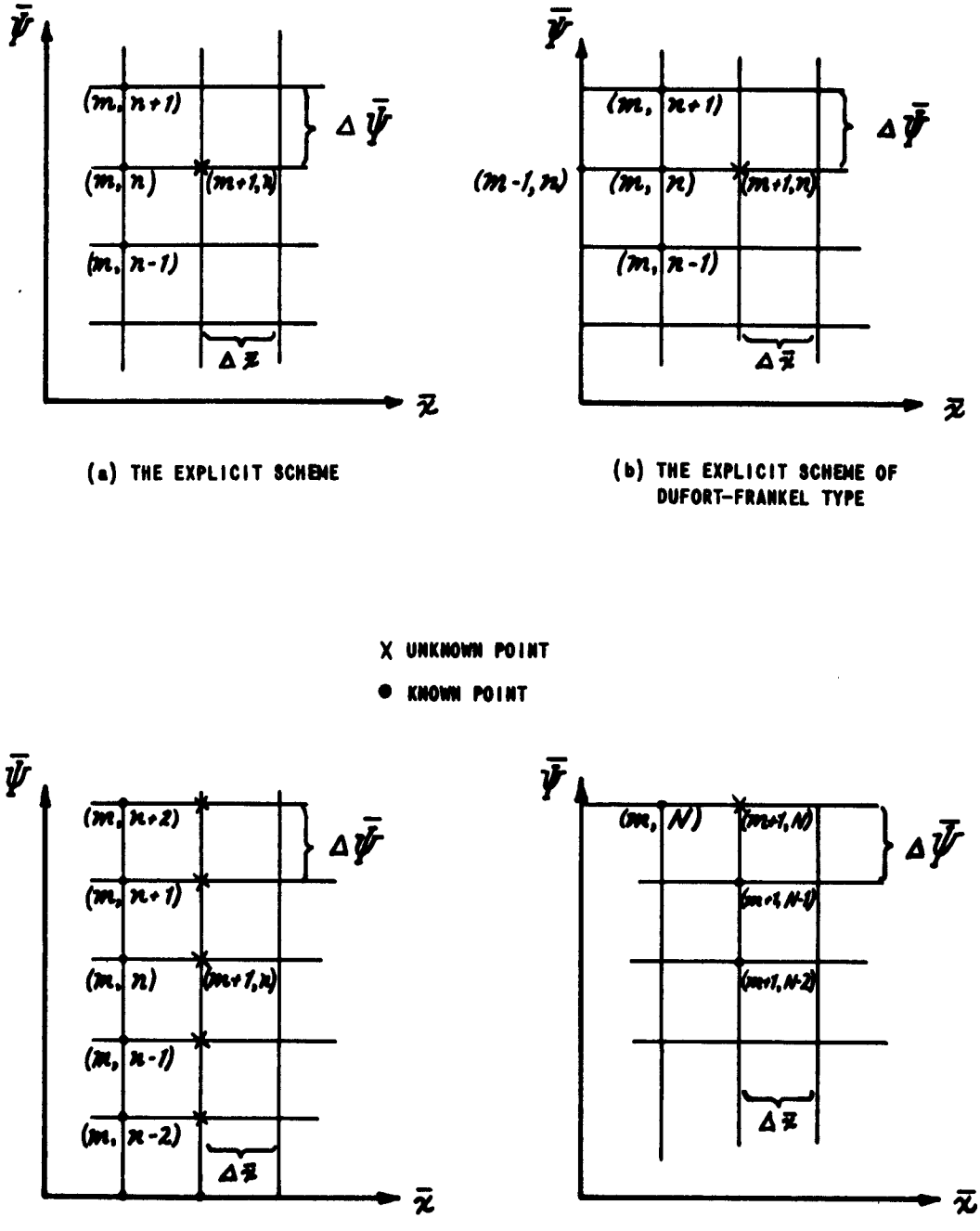

(a) THE EXPLICIT SCHEME

(b) THE EXPLICIT SCHEME OF DUFORT–FRANKEL TYPE

X UNKNOWN POINT

● KNOWN POINT

(c) THE IMPLICIT SCHEME

(d) DIFFERENCE QUOTIENT FOR THE BOUNDARY POINT

Figure 1 SKETCH FOR CONSTRUCTING DIFFERENCE QUOTIENTS

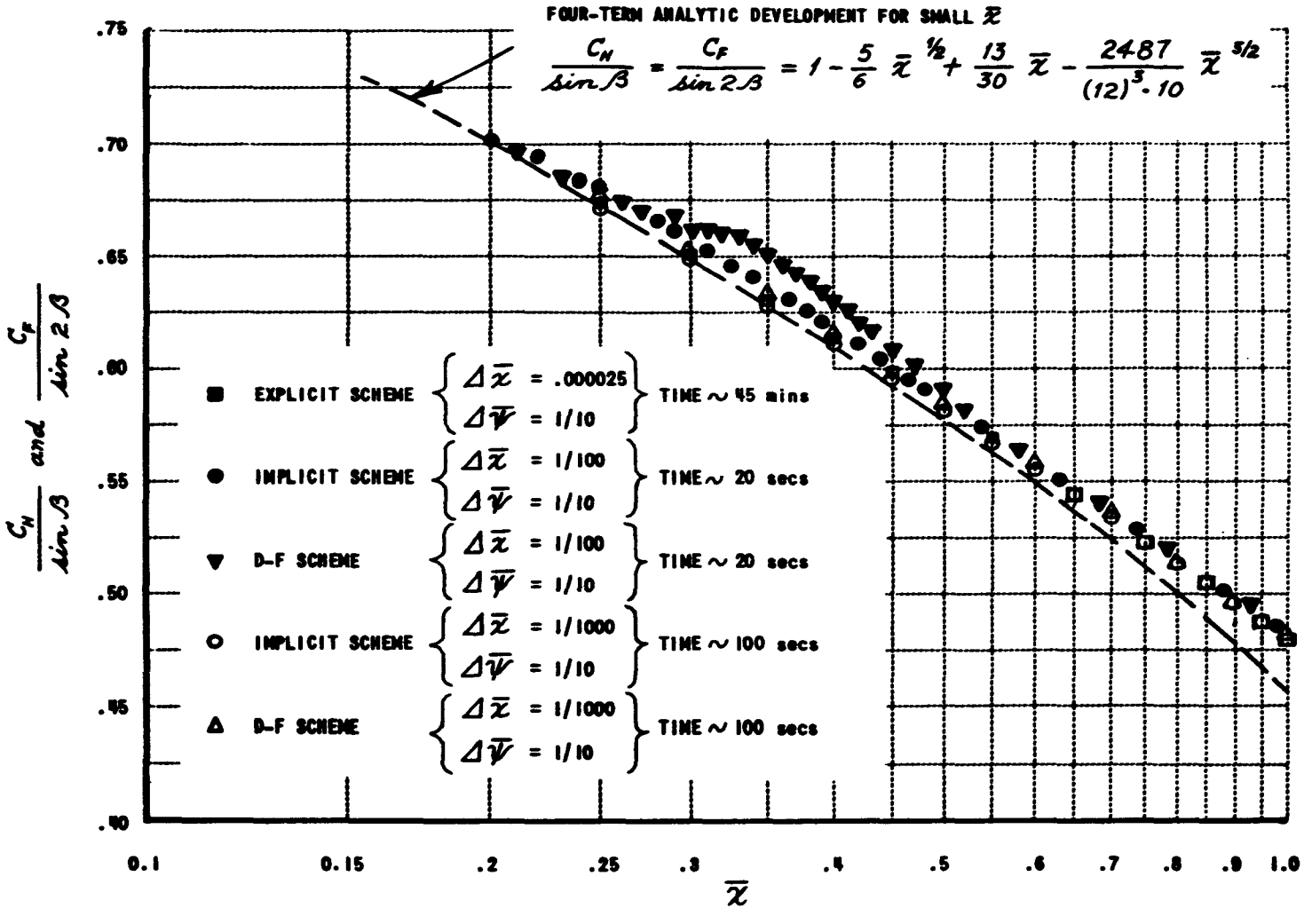

Figure 2 SURFACE HEAT-TRANSFER AND SKIN-FRICTION COEFFICIENTS DETERMINED BY EXPLICIT, IMPLICIT, AND DUFORT-FRANKEL SCHEMES

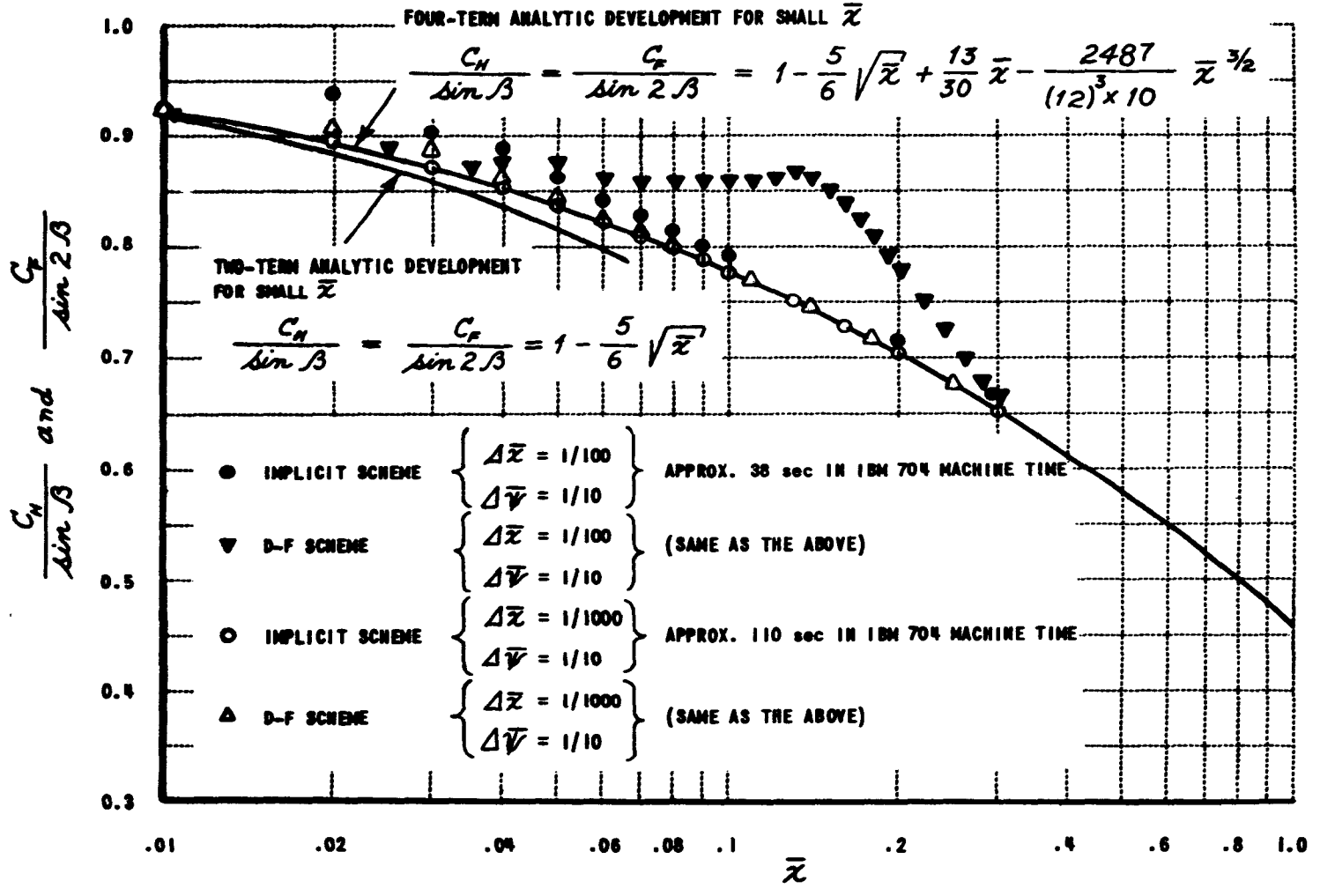

Figure 3 SURFACE HEAT-TRANSFER AND SKIN-FRICTION COEFFICIENTS AS DETERMINED BY THE IMPLICIT AND DUFORT-FRANKEL SCHEMES

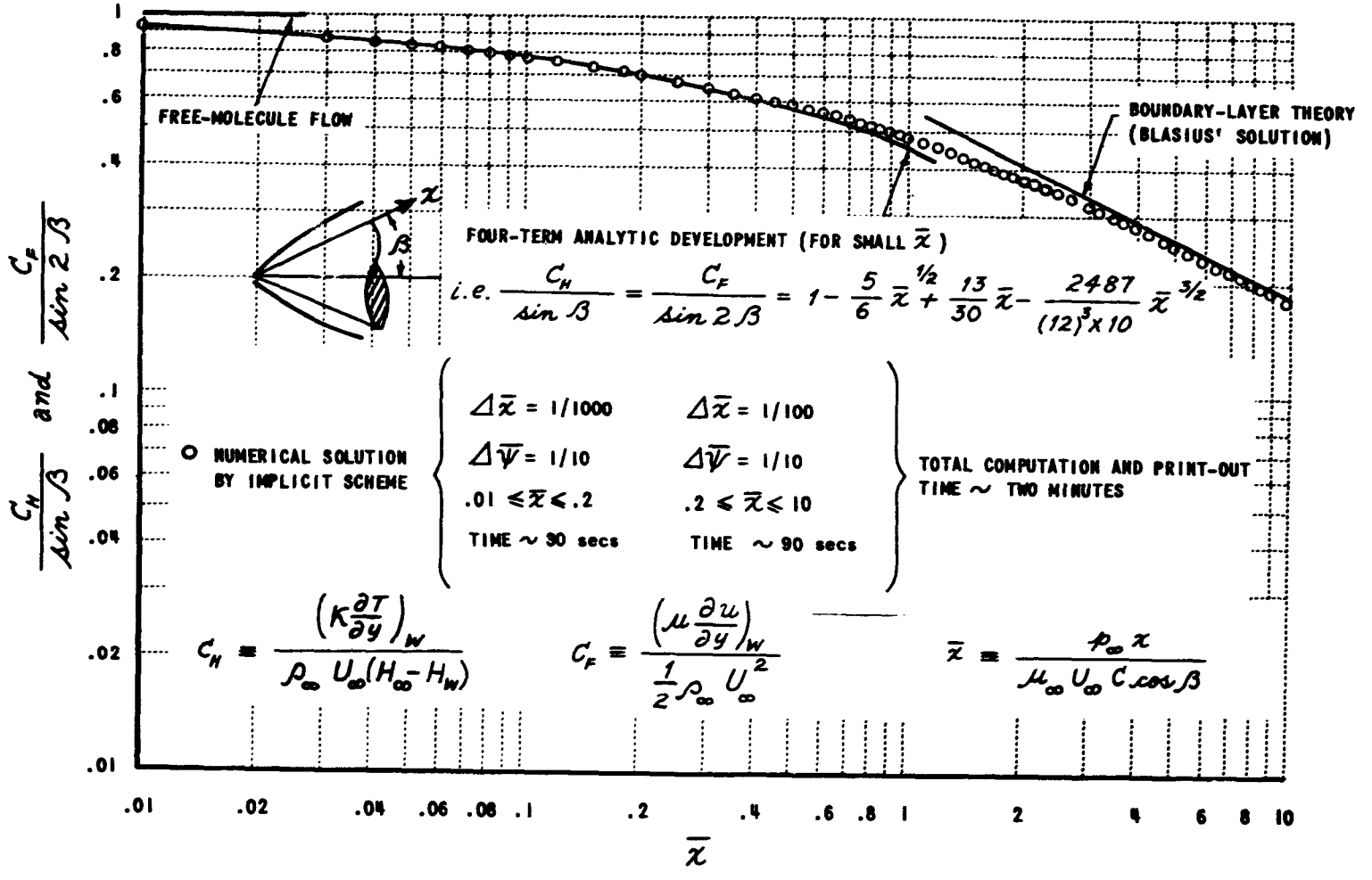

Figure 4 SURFACE HEAT TRANSFER AND SKIN FRICTION AT VARIOUS DEGREES OF GAS RAREFACTION

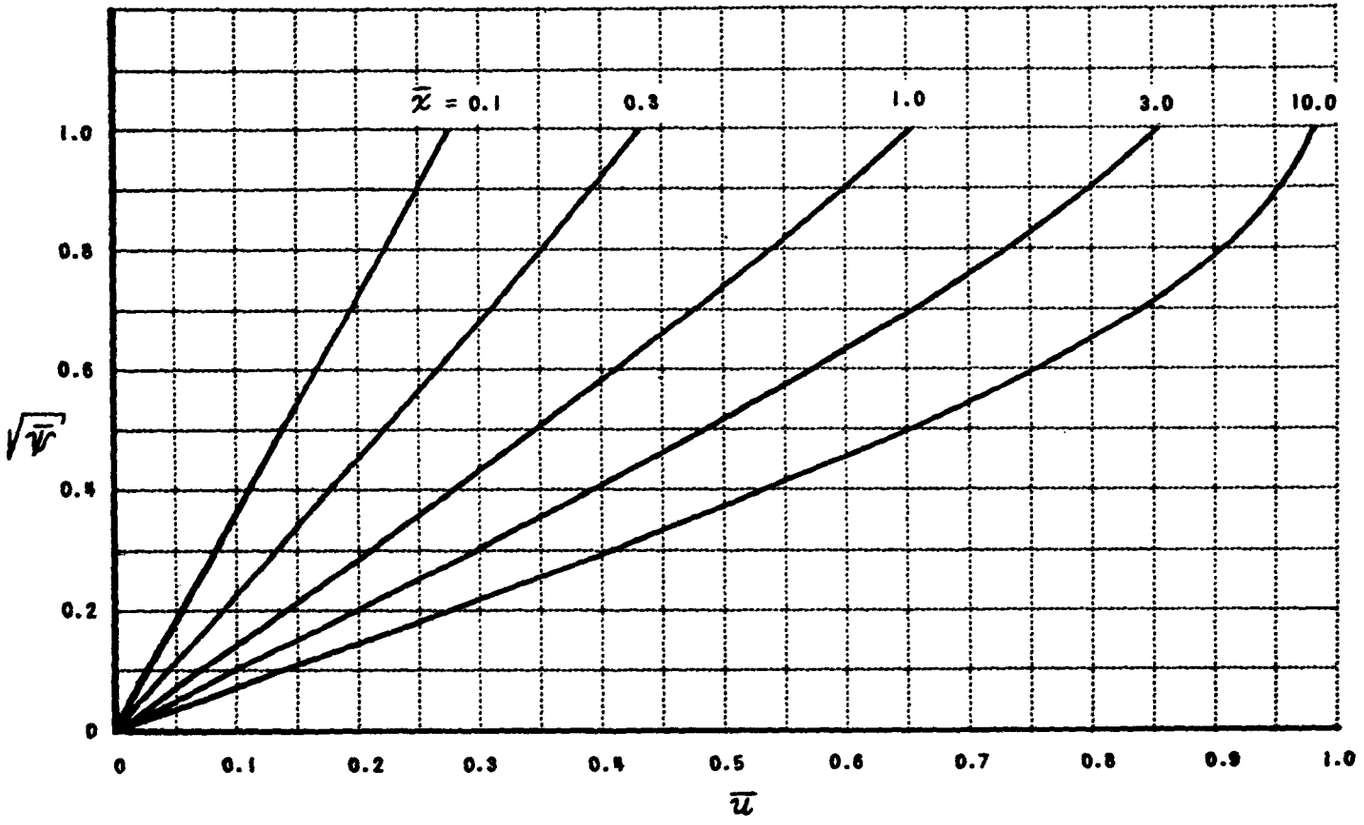

Figure 5 VELOCITY PROFILE OF VISCOUS SHOCK LAYER ON CONE

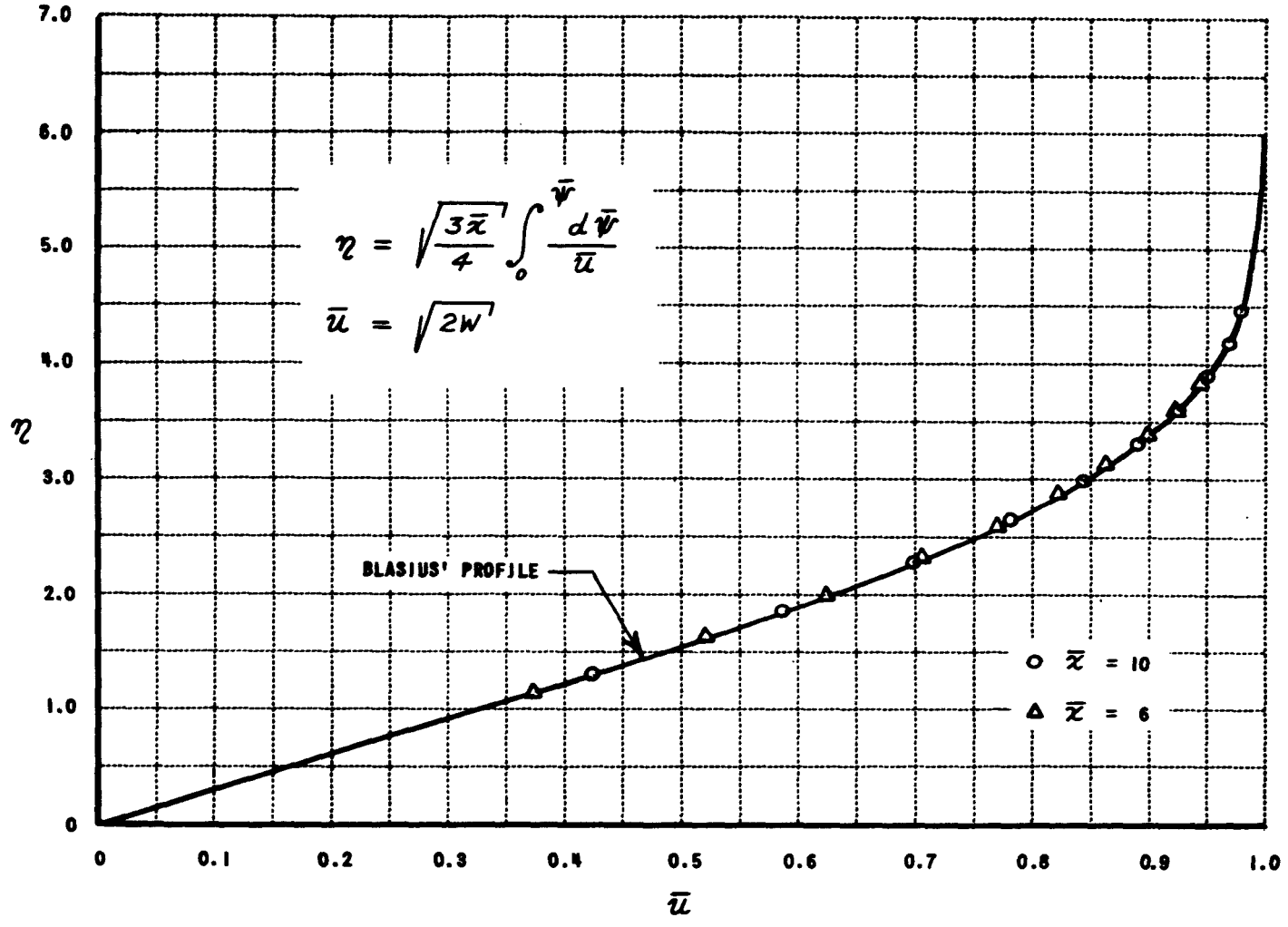

Figure 6 CORRELATION OF VELOCITY PROFILES AT LARGE DISTANCES FROM THE CONE APEX
BLASIUS' PROFILE